Materials Science in Semiconductor Processing 27 (2014) 634–642

Contents lists available at ScienceDirect

Materials Science in Semiconductor Processing

journal homepage: www.elsevier.com/locate/mssp

Template free titania photoanodes modified with carbon black or multi-wall carbon nanotubes: Thermal treatment at low and high temperature for the fabrication of quasi-solid state dye sensitized solar cells

Andreas Rapsomanikis [a], Dimitra Sygkridou [a,b], Dimitrios Karageorgopoulos [a,b], Elias Stathatos [a,*]

[a] Department of Electrical Engineering, Technological-Educational Institute of Western Greece, GR-26334 Patras, Greece
[b] Physics Department, University of Patras, 26500 Patras, Greece

ARTICLE INFO

Keywords:
Multi-wall carbon nanotubes
Carbon black
TiO_2 electrode
Dye-sensitized solar cells
Low temperature
Quasi-solid state electrolyte

ABSTRACT

A simple procedure was developed to prepare modified titania (TiO_2) photoanodes for dye sensitized solar cells at low and high temperature in order to improve overall cell efficiency. Modification of TiO_2 films achieved by the incorporation of either carbon black powder (CBP) or multi-wall carbon nanotubes (MWCNTs). A small quantity of titanium alkoxide was added in a dispersion of titania (TiO_2) powder consisting of nanoparticles at room temperature, which after alkoxide's hydrolysis helps to the connection between titania (TiO_2) particles and to the formation of mechanically stable relatively thick films on conductive glass substrates. The absence of surfactant allowed us to prepare films at relatively low temperature (~100 °C), while the effect of sintering at a higher temperature (500 °C) was also studied. The structural properties of the films were examined with porosimetry method and microscopy analysis. Better electrical results were obtained for the MWCNT (0.1 wt%) modified TiO_2 films, with 3.14% and 4.68% conversion efficiencies under 1 sun illumination after treatment at 100 °C and 500 °C, respectively. The enhancement in photocurrent for MWCNT-TiO_2 films compared to pure TiO_2 films is attributed to the improved interconnectivity between TiO_2 nanoparticles, which further improved the electron transport through the film. For carbon doped CBP-TiO_2 cells, lower efficiencies were observed compared to pure TiO_2.

1. Introduction

Dye sensitized solar cells (DSSCs) have attracted substantial interest as a low-cost alternative to conventional silicon-based solar cells [1]. Titanium dioxide (TiO_2) is one of the most promising semiconductors, which has been extensively studied for environmentally friendly applications, due to its good characteristics of powerful oxidation strength [2], non-toxicity [3], simplicity of fabrication [4], and stability under ambient conditions [5]. Several techniques such as sol–gel, hydrothermal treatment, chemical vapor deposition, electrophoretic deposition and spray pyrolysis can be used to prepare crystalline titanium dioxide [6–11]. Among these preparation methods, sol–gel method is the most widely used [12,13]. So far, the methods that obtain the most-efficient TiO_2 films for

* Corresponding author. Tel./fax: +30 2610 369242.
E-mail address: estathatos@teipat.gr (E. Stathatos).

http://dx.doi.org/10.1016/j.mssp.2014.07.046
1369-8001/

DSSCs have been based on high-temperature calcination but this is also a cost intensive process. In addition, high temperature treatment of TiO_2 films cannot be applied to flexible plastic electrodes. The development of low-temperature fabrication methods could overcome two main problems: (a) the incomplete necking of the particles and (b) the presence of residual organics in the film. These problems cause lower electron diffusion coefficients and electron lifetimes. Apart from calcination temperature, another key parameter is to improve the electronic transport with the incorporation of a very small amount of carbonaceous materials, such as pure carbon powder [14–16], carbon nanotubes (CNT) [17,18] or graphene [19,20], into nanocrystalline TiO_2 films. These materials can be used to enhance charge carriers mobility. The higher electrical conductivity of the carbonaceous materials offers the possibility of increasing photocurrent, thus increasing overall conversion efficiency. Especially, carbon nanotubes are promising materials because of their tubular structure, electrical properties, mechanical strength, thermal stability and high surface area. The introduction of carbon particles or multi-walled tubes (MWCNT), as electrodes in organic solar cells and DSSC has already been carried out. There is a general agreement that MWCNT can efficiently enhance the transport of electrons, besides providing higher electronic conductivity, which confers higher photo-conversion efficiency for these solar cells. However, the introduction of defects/traps due to the decrease in particle size in TiO_2 pure material somehow decreases the efficiency of the cells to some extent although the benefits arising from the use of nanocomposite materials in DSSCs technology are widely reported [21–24]. The chemical diffusion coefficient value for electrons in a nanostructured porous film is three orders of magnitude less than that calculated for bulk materials. This means that charge carrier diffusion may suffer from enhanced probability for charge recombination, mainly in the electrolyte because of the presence of the redox couple [25]. Therefore, the presence of carbon materials in the TiO_2 films could be beneficial for the overall performance of the solar cells.

In this work, we present an easy method for producing modified TiO_2 photoelectrodes without the addition of any organic template at room temperature. According to a previous reported method, P25 powder was dispersed in ethanol without any surfactant [26]. A small amount of titanium isopropoxide was added into the ethanolic solution, which helps the interconnection between TiO_2 particles and enhances the mechanical stability of the film. The as-prepared films were directly modified with either carbon black powder (CBP) or multi-wall carbon nanotubes (MWCNTs) by simple addition of the carbon materials to the starting solution. The films were tested as photoanodes in DSSCs either treated at low or at high temperature.

2. Experimental

2.1. Materials

Carbon black powder (VULCAN-XC72R) was purchased from CABOT. Multi-wall carbon nanotubes (MWCNT), Titanium (IV) isopropoxide (TTIP), Poly (propylene-glycol) bis(2-aminopropyl)ether MW 230, 3-isocyanatopropyl triethoxy silane, 1-methyl-3-propylimidazolium iodide, lithium iodide, iodine, tert-butyl pyridine, guanidine thiocyanate, hydrogen hexachloroplatinate(IV) hydrate (H_2PtCl_6) and all solvents were purchased from Sigma-Aldrich and used as received. Titania powder P25 was provided by Degussa, (Germany, 30% Rutile and 70% Anatase) and di-tetrabutylammonium cis-bis (isothiocyanato) bis(2,2′-bipyridyl-4,4′-dicarboxylato) ruthenium(II)—N-719 was provided by Solaronix. SnO_2:F transparent conductive electrodes (FTO, TEC15) 15 Ω/square were purchased from NSG group, USA. Double distilled water (Mega Pure System, Corning, conductivity: 18.2 μScm^{-1}) was used in all experiments.

2.2. Preparation of the CBP-TiO_2 and MWCNT-TiO_2 photoelectrodes

1 g of P25-TiO_2 powder was added in 10 ml of ethanol followed by magnetic stirring to obtain a homogeneous dispersion. No surfactants were used as templates to the solution. 0.053 M TTIP was added in the previous dispersion under stirring. TTIP concentration was optimum as it was examined in a previous publication [26]. Solution was ultrasonicated for 15 min. For CBP-TiO_2 films, carbon black was added in the solution varying the weight ratio from 0.05 to 1 wt%. MWCNT-TiO_2 films were prepared by the addition of MWCNTs varying from 0.02 to 0.15 wt% into the initial solution.

2.3. Films fabrication and characterization

A home-made dip-coating device was used to dip coat the FTO glass substrate in the sols (with or without the presence of carbon materials) at a withdrawal rate of 12 cm/min to create films with an effective surface area of around 1 cm^2. All films then dried for 1 h at room temperature to prevent the creation of any cracks. The thickness of the pure and modified TiO_2 films was in all cases around 5 μm. After that, films were calcined in a multi-segment programmable furnace (PLF 110/30, Protherm) at a ramp rate of 5 °C/min to 100 °C or alternatively to 500 °C for 30 min and then they cooled down naturally. The nitrogen sorption/desorption isotherms of all samples were measured with a Micromeritics Tristar 3000 and the surface area, porosity, and pore size distribution were derived by differentiating them according to BET method. All samples were degassed for 2 h at 100 °C before N_2 adsorption analysis. The values were obtained from thick films after scratching the material due to the difficulty of sample collection from the thin films. For the visual morphology of nanostructure, an environmental scanning electron microscope (FESEM, Zeiss SUPRA 35VP) was used. Infrared spectroscopy (FTIR) was also studied using a Jasco FTIR-4100 spectrometer.

2.4. Fabrication and characterization of quasi-solid state dye-sensitized solar cell

2.4.1. Dye sensitization of TiO_2 films

The TiO_2 films prepared by the previously described procedure on FTO glass substrates were immersed into a

Please cite this article as: A. Rapsomanikis, et al., Materials Science in Semiconductor Processing (2014), http://dx.doi.org/10.1016/j.mssp.2014.07.046

0.4 mM (ethanol/acetonitrile 50:50 v/v) solution of N-719 dye and were left there for 24 h. The high loaded with dye films were copiously washed with ethanol to remove the excess dye and dried in a stream of nitrogen. Before their use in DSSCs, the electrodes were left in the oven (90 °C) for 15 min to remove any ethanol or humidity that could be present in the pores of the films.

2.4.2. Quasi-solid electrolyte preparation

We used a hybrid organic–inorganic material which was prepared according to a previously reported procedure [27,28]: Poly (propylene glycol) bis (2-aminopropyl ether) 230 MW and 3-isocyanatopropyltriethoxysilane (ICS; molar ratio ICS/diamine=2) were mixed in tetrahydrofuran (THF) under reflux conditions (64 °C) for 6 h. Under such conditions the isocyanate group of ICS reacts with the amino groups of poly-(propylene glycol) bis (2-aminopropyl ether) (acylation reaction), producing urea connecting groups between the polymer units and the inorganic part. After evaporation of THF using rotary evaporator, a viscous precursor was obtained, which was stable at room temperature for several months. The abbreviated name of the precursor used in the present work is ICS-PPG230, referring to molecular weight 230 of the poly-(propylene glycol) oligomer in the hybrid material.

The gel electrolyte was synthesized by the following procedure. 0.175 g of the functionalized alkoxide precursor ICS-PPG230 was dissolved in 0.4 g of sulfolane and 0.2 g of methoxypropionitrile under vigorous stirring. Then 0.092 g glacial acetic acid (AcOH) followed by 0.03 g 1-methyl-3-propylimidazolium iodide (MPII), 0.03 g LiI and 0.015 g I_2 were added. Finally 0.051 g of tert-butyl pyridine (TBP) and 0.0089 g of guanidine thiocyanate (Gu-SCN) were also added. 1-Methyl-3-propylimidazolium iodide was used in order to avoid crystallization of LiI, while the presence of LiI was necessary since these small mobile ions allow increase in ionic conductivity.

After two hours of stirring, one drop of the obtained sol was placed on the top of the titania electrode covered with the dye and a slightly platinized FTO counter electrode was pushed by hand on the top. The platinized FTO glass was made by casting few drops of H_2PtCl_6 solution (5 mg/1 ml of isopropanol) followed by heating at 450 °C for 10 min. The two electrodes tightly stuck together by –Si–O–Si– bonds developed by the presence of ICS-PPG230.

2.4.3. Characterization of the DSSCs

J–V curves were recorded by connecting the cells to a Keithley Source Meter (model 2601) which was controlled by Keithley computer software (LabTracer). Cell active area for these measurements was finally 0.3 cm^2 using an appropriate mask. Illumination intensity was 100 mW/cm^2 coming from a Solar Light Co solar simulator (model 16S-300) equipped with AM 0 and AM 1.5 direct Air Mass filters and a Xe-lamp to simulate solar radiation at the surface of the earth. Cell performance parameters including short-circuit current density (J_{SC}), open circuit voltage (V_{OC}), maximum power (P_{max}), fill factor (*FF*) and overall cell conversion efficiency, were measured and calculated from the *J–V* characteristic curves. Three devices at least were prepared for each CBP-TiO_2, MWCNT-TiO_2 and pure P25-TiO_2 films while their average values are presented in all tables and figures.

3. Results and discussion

3.1. Titania film deposition on FTO conductive glass electrodes

In this work, we examined a straightforward method for relatively thick TiO_2 nanocrystalline films on FTO electrodes without a surfactant template while the effect of film modification with carbon black or multi-wall carbon nanotubes was also examined. The absence of any organic content is of great interest as its presence limits electron diffusion and finally DSSC's overall performance. We varied the concentration of TTIP in P25-TiO_2 solution in terms of the less quantity needed for the formation of stable films on FTO glass substrates. The TTIP/P25-TiO_2 molar ratio was varied from 0–0.1 (always the P25-TiO_2 quantity was kept constant). When the TTIP/P25-TiO_2 molar ratio was less than 0.02, the adherence of the film on the glass was poor. The best adherence of the films was achieved for 0.053 M ratio and hereafter we kept it constant to all experiments. This result is expected as a certain amount of TTIP is needed for the interconnection of P25-TiO_2 particles due to –O–Ti–O– network formation after alkoxide's hydrolysis/condensation in ambient humidity according to the reaction:

$$TiO_2(P25)+nTi(OC_3H_7)_4+2nH_2O\rightarrow(n+1)TiO_2+4nC_3H_7OH$$

Less alkoxide content resulted in poor film adhesion as a large fraction of the TiO_2 film was peeled off the substrate. On the other hand, higher alkoxide content in the sol could create more amorphous TiO_2 phases in films due to the presence of untreated TTIP and as a consequence we could obtain poorer performance of the DSSC. Therefore, it seems reasonable that the amount of TiO_2 to be formed from TTIP has to be significantly much less than the amount of P25-TiO_2 added as nanocrystalline powder dispersion in EtOH. All films were made by dip-coating in a speed of 12 cm/min. The durability of the films in water rinsing (sometimes violently) was very strong. In the presence of carbon black or MWCNTs the adhesion of the composite films on FTO glass was also very strong while the durability is comparable with that measured for pure TiO_2 films. The durability of composite films was checked for a variety of carbon black or MWCNTs quantities and the results were similar in all cases.

3.2. Structural properties of pure and modified TiO_2 films

As the porosity of TiO_2 films is one of the basic features needed to construct efficient photoelectrodes for dye adsorption, the as-prepared pure or modified TiO_2 films were examined with N_2 sorption–desorption analysis in order to determine their textural properties. The measurements were carried out on powder which was carefully scratched from thick films. The N_2 sorption–desorption

Please cite this article as: A. Rapsomanikis, et al., Materials Science in Semiconductor Processing (2014), http://dx.doi.org/10.1016/j.mssp.2014.07.046

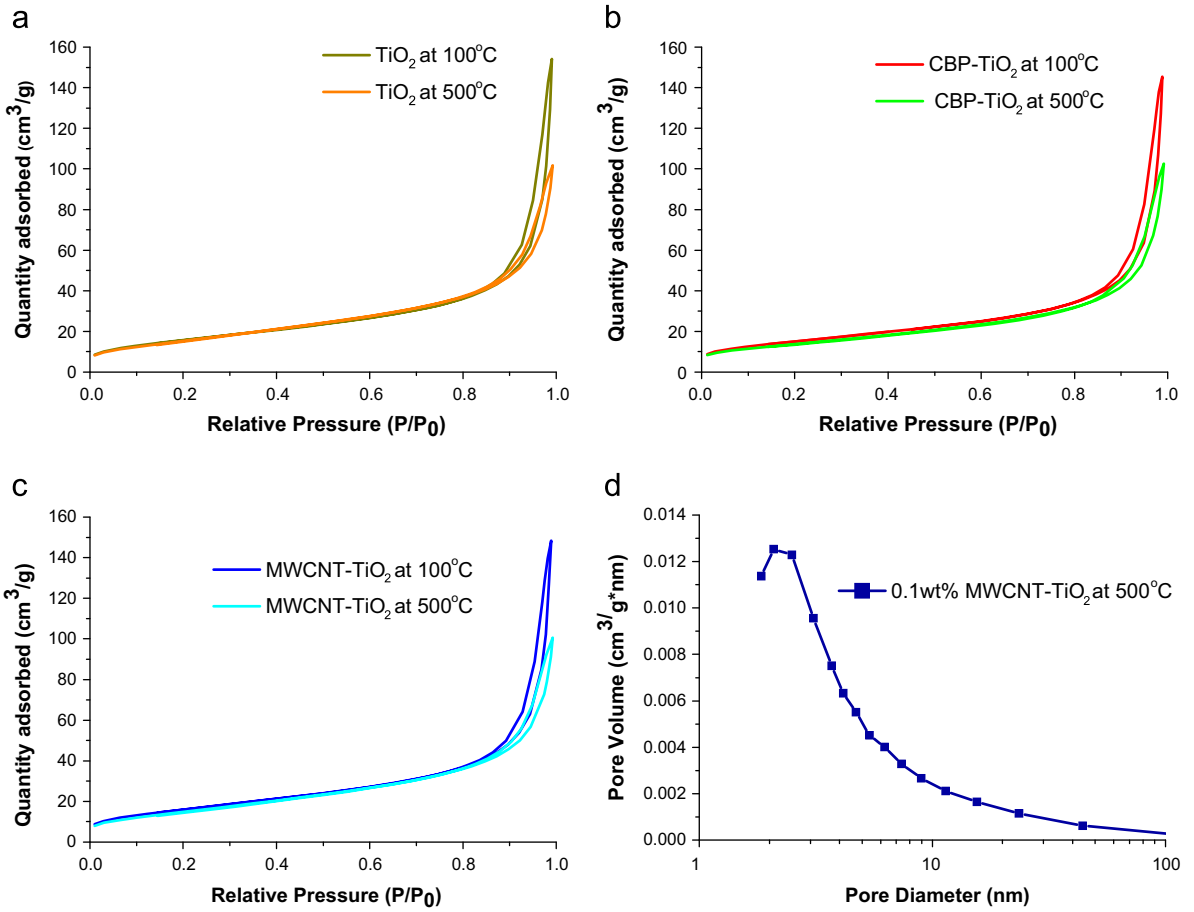

Fig. 1. Sorption–desorption isotherms for optimized (a) pure P25-TiO_2, (b) CBP-P25-TiO_2 and (c) MWCNT-P25-TiO_2 at low and high temperature. Pore size distribution (MWCNT-P25-TiO_2) measured at 500 °C is presented as figure (d).

isotherms of the as-prepared TiO_2 film at relatively low temperature (100 °C) with a 0.053 M TTIP molar ratio in P25-TiO_2 powder are presented in Fig. 1a. The hysteresis loop appears in relatively a high pressure region ($0.8 < P/P_0 < 1.0$), which suggests that Degussa P25 particles could lead to the formation of larger pores. The shape of the isotherms is typical for mesoporous materials. The Brunauer, Emmett and Teller (BET) specific surface area and Barrett, Joyner and Halenda (BJH) pore volume of the as-prepared films were relatively high at 57.8 m^2/g and 0.24 cm^3/g, respectively. In the presence of 0.5 wt% carbon black or 0.1 wt% MWCNTs in TTIP/P25-TiO_2 films at 100 °C the results were almost similar as those that appear in Table 1. In particular, the specific surface area for MWCNT/TTIP/P25-TiO_2 is a little higher (58.9 m^2/g) than that measured for pure TTIP/P25-TiO_2 which is rather expected because of the presence and specific nature of nanotubes in films. The pore diameter varied from 15.4–16.6 nm for pure and carbon treated films. Such large pores are expected to have a beneficial effect on the electrolyte solution wetting and filling in the TiO_2 films. When we decided to heat the as-prepared pure and carbon modified films at high temperature we faced a decrease to all structural characteristics of the films namely total pore volume, specific surface area and pore diameter as it was expected because of the sintering (Table 1). However, the maximum measured decrease was 33% in total pore volume, 13% in specific surface area, 20% in total porosity and 38% in mean pore diameter. As an example, the pore size distribution plot for high temperature prepared 0.1% MWCNT/TTIP/P25-TiO_2 film (Fig. 1d) showed an average pore size of 10.5 nm.

FT-IR studies of the TTIP/P25-TiO_2 film at 100 °C show the characteristics of the formation of high-purity material while similar behavior was monitored for MWCNT/TTIP/P25-TiO_2 and CBP/TTIP/P25-TiO_2 films at the same temperature. The FT-IR spectrum of Fig. 2 clearly shows the peaks corresponding to TiO_2. Peaks located in the area of 400–650 cm^{-1} correspond to the vibration of Ti–O and Ti–O–O bonds. On the other hand, the absence of peaks at 1000 cm^{-1} proves the absence of peroxo groups. Furthermore, FT-IR spectrum firmly suggests the presence of –OH groups which is absolutely necessary for dye adsorption in DSSCs' fabrication. Thus the as-prepared TTIP/P25-TiO_2, MWCNT/TTIP/P25-TiO_2 and CBP/TTIP/P25-TiO_2 films after washing with pure water consisted of pure TiO_2 particles without any significant organic contaminants, which is an important advantage in the evaluation of DSSCs' efficiency made with these TiO_2 electrodes. However, in the case of MWCNT/TTIP/P25-TiO_2 and CBP/TTIP/P25-TiO_2 films there

Please cite this article as: A. Rapsomanikis, et al., Materials Science in Semiconductor Processing (2014), http://dx.doi.org/10.1016/j.mssp.2014.07.046

Table 1
Structural properties of carbon free, CBP-TiO_2 and MWCNTs-TiO_2 films at low and high temperatures.

Temperature (°C)	Sample	Total pore volume V_p (cm^3/g)	Specific surface area S (m^2/g)	Total porosity (%)	Mean pore diameter D_{por} (nm)	Roughness factor (μm^{-1})[a]
100	TiO_2-P25	0.24	57.8	47.7	16.2	2.05
	0.5%CBP/ TiO_2-P25	0.22	54.5	45.5	16.6	2.85
	0.1%MWCNT/ TiO_2-P25	0.23	58.9	46.6	15.4	2.47
500	TiO_2-P25	0.16	57.9	37.8	10.2	1.56
	0.5%CBP/ TiO_2-P25	0.16	49.8	37.8	12.9	2.89
	0.1%MWCNT/ TiO_2-P25	0.16	55.8	37.8	10.5	1.82

[a] Roughness factor was obtained by multiplying the specific surface area and TiO_2 weight.

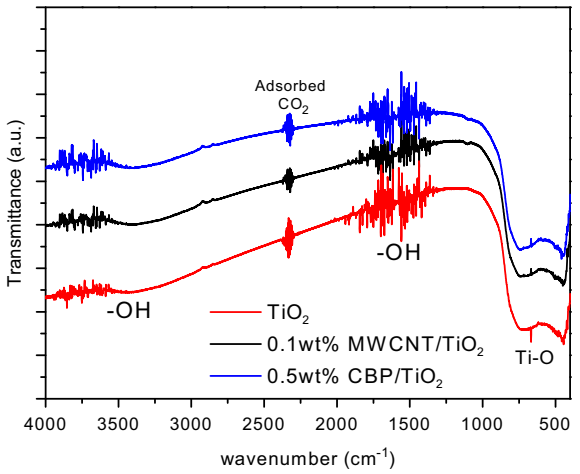

Fig. 2. FTIR spectra of pure P25-TiO_2, CBP and MWCNT in optimum quantities annealed at 100 °C.

was no peak related to the reaction of MWCNT and CBP with P25-TiO_2 host material.

The films with optimum TTIP content (0.053M), 0.5 wt% CBP/TTIP/P25-TiO_2 and 0.1 wt% MWCNT/TTIP/P25-TiO_2 were examined with a microscopy technique (FESEM) to determine the homogeneity of the films and collaboration among carbon and P25-TiO_2 particles. In Fig. 3a, FESEM analysis shows that the TiO_2 film consisted of 25–30 nm particles uniformly distributed in film. The thickness of the film, which is an important parameter for the evaluation of dye-sensitized solar cell efficiency constructed with this film, was measured to be approximately 5 μm. Film thickness was not affected by CBP or MWCNT modification as this quantity even at its higher value, was very low compared to P25-TiO_2 content. In case of CBP modification (Fig. 3b) larger particles of carbon were homogeneously dispersed in nanocomposite TiO_2 host material while there is a good connection among them. Finally, when carbon nanotubes were introduced in films the characteristic shape of the nanotubes appear in FESEM images while no serious deviations to the film shape and homogeneity compared to pure TTIP/P25-TiO_2 were detected.

Fig. 4 shows the absorbance of N-719 dye after detachment from all TiO_2 films exposed to 1 M NaOH for 10 min. The concentration of the adsorbed dye was calculated using the absorption values and the molar extinction coefficient of N-719 dye and was found to range between 0.00588 mM and 0.0354 mM [29,30]. It is obvious that the quantity of the dye detached from untreated P25-TiO_2 samples is higher than those detected for CBP or MWCNT modified samples. In contrary to the structural properties characterized with porosimetry measurements the CBP/P25-TiO_2 films seem to absorb more quantities of the N-719 dye while the MWCNT/P25-TiO_2 films showed the poorest absorption capacity among the three different films. However, for all cases of films the temperature increase seems to be effective to the dye's adsorption capacity. This can be attributed to the water content of the TiO_2 films which significantly diminishes with annealing temperature, indicating that samples annealed at 100 °C retain much more water than samples annealed at higher temperatures.

3.3. Characterization of the dye-photoelectrochemical solar cell performance

The as-prepared pure TiO_2 or carbon black, multi-wall carbon nanotubes modified films on FTO glass substrates were examined as negative photoelectrodes in quasi solid-state dye-sensitized solar cells. The corresponding characteristic *J–V* parameters for a variety of carbon black and multi-wall carbon nanotubes concentrations in relation to the TiO_2 are presented in Table 2. For films heated at low temperature (100 °C) the maximum overall efficiency was obtained as 0.5 wt% CBP and 0.1 wt% for multi-wall carbon nanotubes in the solution compared with TiO_2 weight content. However, in the case of CBP the overall efficiency was always lower than pure TiO_2 films while in the case of multi-wall carbon nanotubes for 0.1 wt% a 6% increase was observed. The current density–voltage (*J–V*) characteristic curves of quasi solid-state dye sensitized solar cells for low temperature TiO_2 films with variable CBP and MWCNT content prepared on FTO substrates are presented in Fig. 5a and b, respectively. It is worth noting that in case of CBP modified films when the concentration of carbon was high the electrical characteristics of the cells were rapidly decreased.

Additionally, the efficiencies of the cells with the previous as-prepared pure and modified films sintered at

Please cite this article as: A. Rapsomanikis, et al., Materials Science in Semiconductor Processing (2014), http://dx.doi.org/10.1016/j.mssp.2014.07.046

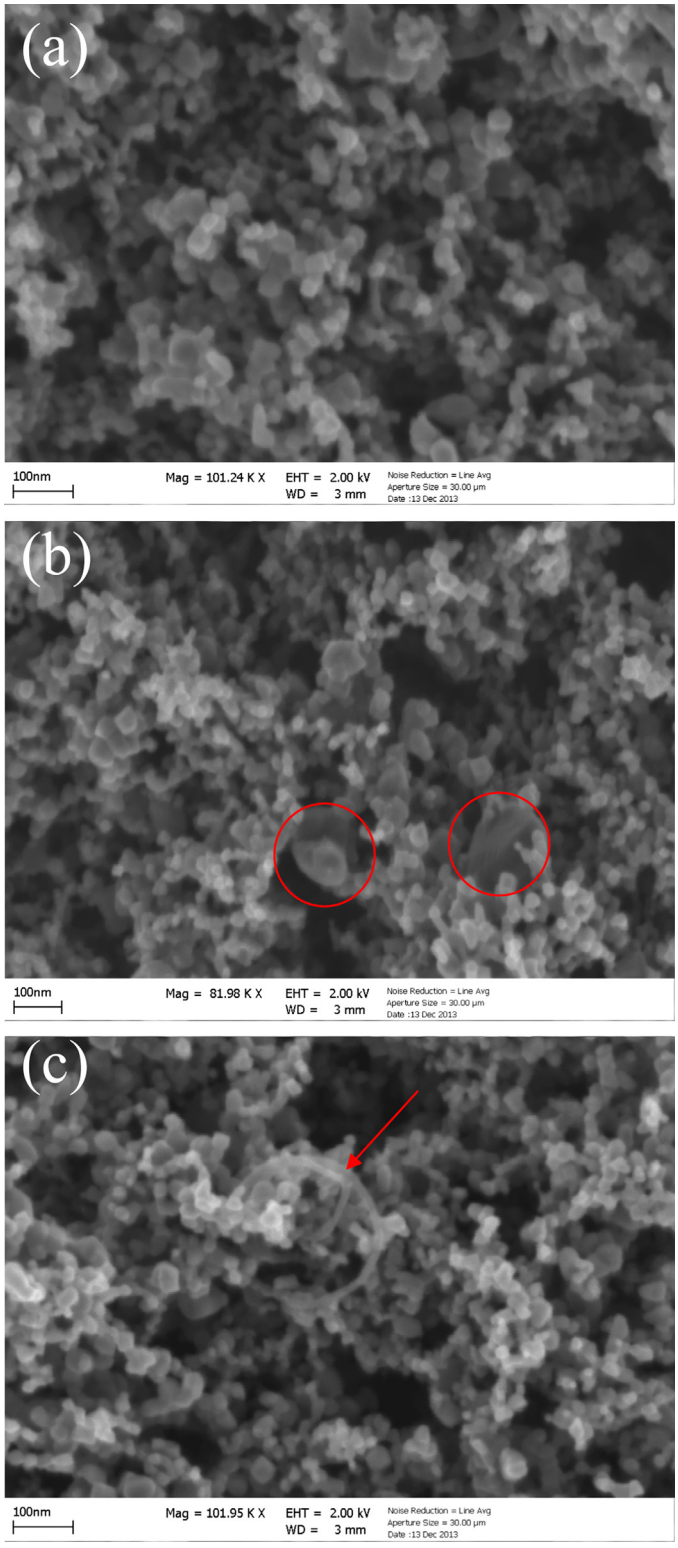

Fig. 3. SEM images of (a) pure P25-TiO_2, (b) CBP and (c) MWCNT in optimum quantities annealed at 500 °C.

high temperature (500 °C) were also examined (Table 2). In all cases the efficiencies of the cells were increased which was an expected result as TiO_2 particles treated at high temperature give improved charge collection efficiencies because of firm necking between them and crystallization of TiO_2 content due to the presence of TTIP

Please cite this article as: A. Rapsomanikis, et al., Materials Science in Semiconductor Processing (2014), http://dx.doi.org/10.1016/j.mssp.2014.07.046

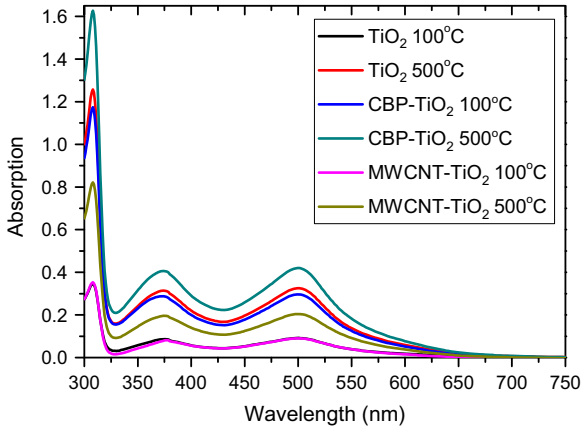

Fig. 4. UV–vis absorption of dye N-719 detached from pure P25-TiO_2 samples and CBP or MWCNT modified films after exposed in 1 M NaOH.

Table 2
Cell performances measured for CBP-TiO_2 and MWCNTs-TiO_2 for different weight ratios measured at 100 mW/cm^2 and AM 1.5 simulated solar light.

Sample	Temperature (°C)	Weight ratio (%)	J_{sc} (mA/cm^2)	V_{oc} (mV)	*FF*	*n* (%)
CBP-TiO_2	100	0	5.85	0.71	0.71	2.97
		0.05	2.35	0.68	0.64	1.01
		0.1	1.83	0.64	0.66	0.76
		0.2	2.42	0.63	0.58	0.86
		0.5	3.38	0.71	0.71	1.69
		1.0	2.52	0.45	0.31	0.35
	500	0	7.60	0.71	0.67	3.56
		0.05	7.18	0.67	0.68	3.29
		0.1	7.43	0.61	0.73	3.31
		0.2	7.43	0.64	0.63	3.01
		0.5	7.27	0.59	0.68	2.92
		1.0	2.81	0.51	0.63	0.90
MWCNT-TiO_2	100	0	5.85	0.71	0.71	2.97
		0.02	3.80	0.67	0.73	1.86
		0.05	5.92	0.69	0.71	2.90
		0.10	6.79	0.70	0.66	3.14
		0.15	5.59	0.66	0.69	2.53
	500	0	7.60	0.71	0.67	3.56
		0.02	8.37	0.71	0.65	3.86
		0.05	8.16	0.72	0.65	3.80
		0.10	11.1	0.70	0.61	4.68
		0.15	8.45	0.67	0.62	3.51

while carbon connection with TiO_2 particles is also improved. The current density–voltage (*J–V*) characteristic curves of quasi solid-state dye sensitized solar cells at high temperature TiO_2 films with variable CBP and MWCNT content prepared on FTO substrates are presented in Fig. 6a and b, respectively. However, the disadvantage of somewhat lower efficiencies obtained at low temperature is overcome by the lower anticipated cost of preparation for the TiO_2 electrode. In case of CBP there is no evidence for better performance in comparison with pure TiO_2 while in the case of the presence of MWCNT in variable quantities in modified films the measured efficiencies were always higher than that obtained for pure TiO_2 film. This means that the electrical conductivity in the films was improved as there is no direct correlation with the

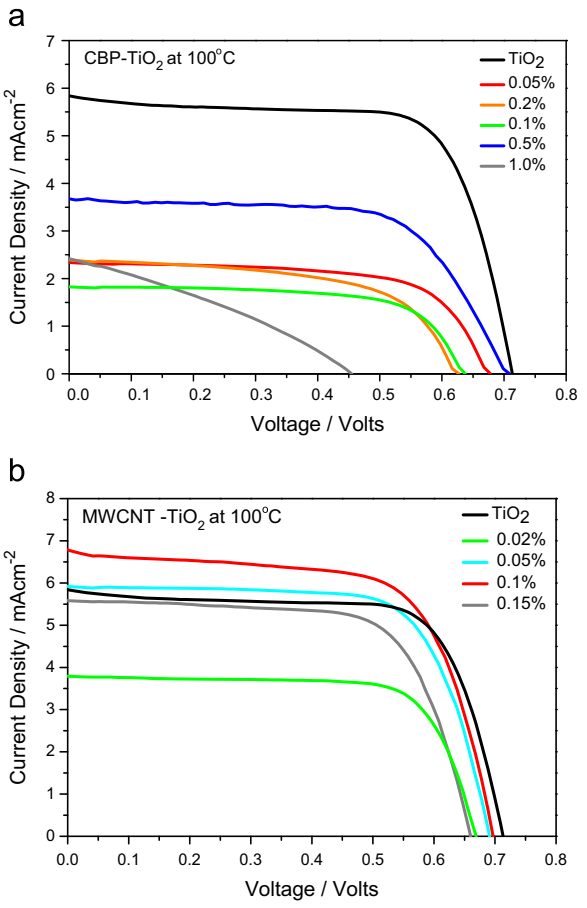

Fig. 5. Photocurrent–voltage curves of DSSCs based on (a) CBP and (b) MWCNT treated TiO_2 nanocrystalline films annealed at low temperature (100 °C)

structural properties of the films which are not improved in the case of MWCNT modification. However, an unexpected behavior with rapid degradation of the cells' electrical characteristics based on 1 wt% CBP/TiO_2-P25 electrodes for both cases of treated at low or elevated temperatures was observed. We believe that this behavior may be due to excess of CBP which results in a less compact TiO_2 layer, where large pores form at the micron scale or quite disconnected aggregates of CBP covered by TiO_2 nanoparticles. Moreover, the decrease in the open circuit voltage can be a result of a decrease in the band offset (energetic difference between the TiO_2 conduction band edge and the iodine/iodide redox potential) or because of an increased recombination rate constant (photoinjected electrons with dye cations and/or tri-iodide species in the electrolyte). The acceleration in the recombination reaction can be confirmed by looking at the *J–V* curves in the dark (Fig. 7). The electron/hole recombination at low and high temperatures for all treated photoelectrodes was examined by measuring the dark current characteristic curves (Fig. 7). In the case of the presence of CBP in the TiO_2 matrix, there is an increase in the dark current values whether the films were treated at low or at high temperatures. The acceleration in the recombination reaction is more intense for

Please cite this article as: A. Rapsomanikis, et al., Materials Science in Semiconductor Processing (2014), http://dx.doi.org/10.1016/j.mssp.2014.07.046

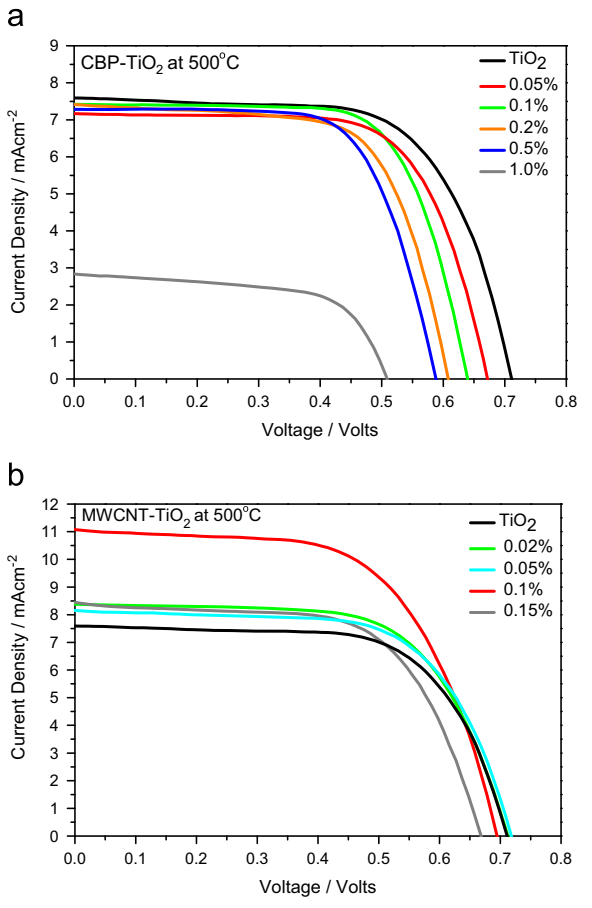

Fig. 6. Photocurrent–voltage curves of DSSCs based on (a) CBP and (b) MWCNT treated TiO_2 nanocrystalline films annealed at high temperature (500 °C).

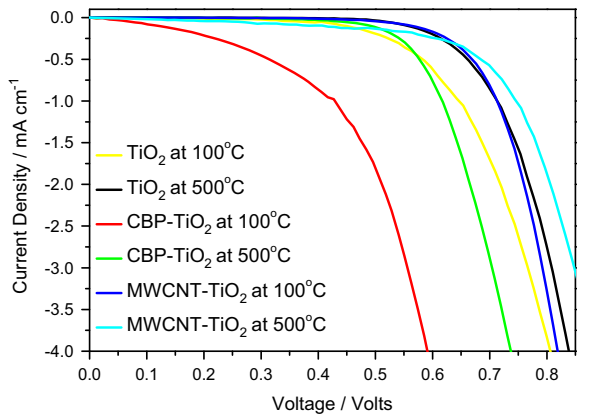

Fig. 7. Dark current–voltage characteristic curves of dye-sensitized solar cells based on pure and carbon modified P25-TiO_2 photoelectrodes annealed at low and high temperature.

photoelectrodes treated at low temperature mainly due to the presence of some content of amorphous TiO_2 from TTIP in addition to the carbon black content. The same behavior was observed for pure and MWCNT modified P25-TiO_2 samples treated at low temperature. This is a negative effect especially when using gel electrolytes where decay in the V_{oc} values is expected due to a large concentration of poly-iodides species. However, in the case of MWCNT modified P25-TiO_2 films a lower recombination rate was monitored which is mainly attributed to the presence of multi-wall carbon nanotubes helping the electron transport because of the improved interconductivity between TiO_2 and MWCNT.

4. Conclusion

P25-TiO_2 photoanodes at low and elevated temperatures modified with CBP or MWCNT were prepared by the direct mixing method and characterized by different techniques without any template. DSSCs based on these composite photoelectrodes were also assembled and electrically characterized. Results showed that the incorporation of MWCNT into the TiO_2 working electrode efficiently improved the performance of DSSC either at low or elevated temperatures. The TiO_2 electrode containing 0.1 wt% of MWCNT provided the best electrical parameters: J_{sc} of 6.79 mA cm^{-2} (at 100 °C) and 11.1 mA cm^{-2} (at 500 °C), V_{oc} of 0.70 V (both at 100 °C and 500 °C), and conversion efficiencies of 3.14% (at 100 °C) and 4.68% (at 500 °C). Compared with DSSC based on the conventional TiO_2 porous films, devices based on the composite photoanode exhibited an increase of approximately 16% (at 100 °C) and 46% (at 500 °C) in J_{sc}. The enhancement in photocurrent is attributed to the improved interconnectivity between TiO_2 nanoparticles and MWCNT, which further improved the electron transport through the film. This could be further proved by the lower absorbance of the N-719 dye in the composite film compared with the untreated film where a lower overall efficiency could be expected. At higher carbon nanotube concentrations in the composite electrode a decrease in energy conversion efficiency of the DSSC was monitored, which might be related to the poorer light transmittance at higher MWCNT loading in the composite films and possibly a higher charge recombination, as evidenced by the dark currents. However, the use of carbon black in variable concentrations in P25-TiO_2 films resulted in lower efficiency in all cases.

Acknowledgments

This research has been co-financed by the European Union (European Social Fund – ESF) and Greek National Funds through the Operational Program "Education and Lifelong Learning" of the National Strategic Reference Framework (NSRF) – Research Funding Program: ARCHIMEDES III, investing in knowledge society through the European Social Fund.

References

[1] A. Hagfeldt, G. Boschloo, L. Sun, L. Kloo, H. Pettersson, Chem. Rev. 110 (2010) 6595–6663.
[2] M.I. Litter, Appl. Catal. B: Environ. 23 (1999) 89–114.
[3] H. Choi, E. Stathatos, D.D. Dionysiou, Desalination 202 (2007) 199–206.
[4] V.A. Sakkas, Md.A. Islam, C. Stalikas, T.A. Albanis, J. Hazard. Mater. 175 (2010) 33–44.
[5] J. Gong, J. Liang, K. Sumathy, Renew. Sustain. Energy Rev. 16 (2012) 5848–5860.
[6] E. Stathatos, P. Lianos, Adv. Mater. 19 (2007) 3338–3341.

[7] H. Tong, N. Enomoto, M. Inada, Y. Tanaka, J. Hojo, Electrochim. Acta 130 (2014) 329–334.
[8] K.E. Kim, S.-R. Jang, J. Park, R. Vittal, K.-J. Kim, Sol. Energy Mater. Sol. Cells 91 (2007) 366–370.
[9] W. Jarernboon, S. Pimanpang, S. Maensiri, E. Swatsitang, V. Amornkitbamrung, Thin Solid Films 517 (2009) 4663–4667.
[10] C. Dwivedi, V. Dutta, Adv. Nat. Sci.: Nanosci. Nanotechnol. 3 (2012) 015011.
[11] N. Yang, J. Zhai, D. Wang, Y. Chen, L. Jiang, ACS Nano 4 (2010) 887–894.
[12] M.A. Khan, M.S. Akhtar, O-Bong Yang, Sol. Energy 84 (2010) 2195–2201.
[13] Y. Chen, E. Stathatos, D.D. Dionysiou, J. Photochem. Photobiol. A: Chem. 203 (2009) 192–198.
[14] L. Jun, L. Zhen, L. Kangbao, W. Aixiang, Funct. Mater. Lett. 6 (2013) 1350017.
[15] S.H. Kang, J.Y. Kim, Y.E. Sun, Electrochim. Acta 52 (2007) 5242–5250.
[16] S.H. Kang, J.-Y. Kim, Y.-K. Kim, Y.-E. Sung, J. Photochem. Photobiol. A: Chem. 186 (2007) 234–241.
[17] J.G. Yu, J.J. Fan, B. Cheng, J. Power Sour. 196 (2011) 7891–7898.
[18] A. de Morais, L.M.D. Loiola, J.E. Benedetti, A.S. Gonçalves, C.A. O. Avellaneda, J.H. Clerici, M.A. Cotta, A.F. Nogueira, J. Photochem. Photobiol. A: Chem. 251 (2013) 78–84.
[19] N.L. Yang, J. Zhai, D. Wang, Y.S. Chen, L. Jiang, ACS Nano 4 (2010) 887–894.
[20] M. Zhu, X. Li, W. Liu, Y. Cui, J. Power Sour. 262 (2014) 349–355.
[21] S. Lee, I.-S. Cho, J.H. Lee, D.H. Kim, D.W. Kim, J.Y. Kim, H. Shin, J.-K. Lee, H.S. Jung, N.-G. Park, K. Kim, M.J. Ko, K.S. Hong, Chem. Mater. 22 (2010) 1958–1965.
[22] L.-Y. Liang, S.-Y. Dai, L.-H. Hu, J. Dai, W.-Q. Liu, Wuli Xuebao/Acta Phys. Sin. 58 (2009) 1338–1343.
[23] K. Zhu, N. Kopidakis, N.R. Neale, J. van de Lagemaat, A.J. Frank, J. Phys. Chem. B 110 (2006) 25174–25180.
[24] M.J. Cass, A.B. Walker, D. Martinez, L.M. Peter, J. Phys. Chem. B 109 (2005) 5100–5107.
[25] D.-W. Park, Y. Jeong, J. Lee, J. Lee, S.-H. Moon, J. Phys. Chem. C 117 (2013) 2734–2739.
[26] E. Stathatos, Y. Chen, D.D. Dionysiou, Sol. Energy Mater. Sol. Cells 92 (2008) 1358–1365.
[27] E. Stathatos, Ionics 11 (2005) 140–145.
[28] E. Stathatos, P. Lianos, U.L. Stangar, B. Orel, P. Judeinstein, Langmuir 16 (2000) 8672–8676.
[29] C. Sahin, Th. Dittrich, C. Varlikli, S. Icli, M.Ch. Lux-Steiner, Sol. Energy Mater. Sol. Cells 94 (2010) 686–690.
[30] A. Fillinger, B.A. Parkinson, J. Electrochem. Soc. 146 (1999) 4559–4564.

Please cite this article as: A. Rapsomanikis, et al., Materials Science in Semiconductor Processing (2014), http://dx.doi.org/10.1016/j.mssp.2014.07.046